Heliyon 10 (2024) e24515

Contents lists available at ScienceDirect

Heliyon

journal homepage: www.cell.com/heliyon

Research article

Characterizations and molecular docking mechanism of the interactions between peptide FDGDF (Phe-Asp-Gly-Asp-Phe) and SOD enzyme☆

C.H.E.N. Wen-Tao [a,*], Ying-Yang Zhang [a], Qiang Qiang [b], Ping Zou [a], Ying Xu [a], Chengjun Sun [a], Iftikhar Hussain Badar [c,d]

[a] *School of Biological and Food Engineering, Changzhou University, Changzhou, Jiangsu, 213164, China*
[b] *Changzhou Wujin No. 3 People's Hospital Changzhou, Jiangsu,150030, China*
[c] *Department of Meat Science and Technology, University of Veterinary and Animal Sciences, Lahore 54000, Pakistan*
[d] *College of Food Science, Northeast Agricultural University, Harbin, Heilongjiang 150030, China*

A R T I C L E I N F O

Keywords:
Beef crude proteins
Binding sites
Molecular docking
SPR

A B S T R A C T

In this study, we investigated the antioxidant properties of dry-cured beef crude peptide (BPH) at different storage periods. The combination characteristics of different concentrations of Phe-Asp-Gly-Asp-Phe (FDGDF) and superoxide dismutase (SOD) at different temperatures were analyzed by ultraviolet–visible spectroscopy, fluorescence spectroscopy, and FT-IR spectroscopy, combined with the detection of a SOD activity detection box. It was found that FDGDF could improve the activity of SOD by changing its secondary structure. Bonds were formed at O32/O40/O52 using quantum chemical simulation calculations, and the Fukui index was higher than that of most atoms, indicating that these atoms were more likely to participate in the reaction. SPR biological force analysis showed that FDGDF and SOD were in a fast binding and dissociation mode. This study revealed the theoretical basis for studying the antioxidant mechanism of dry-cured beef and provided ideas for developing new dry-cured beef products.

1. Introduction

Meat products, due to the abundance of proteins, essential fatty acids, vitamins, and minerals, are a vital part of the daily human diet [1]; however, these meat components are prone to specific degradative changes affecting proteins, lipids, pigments, and vitamins, leading to sensory degradation of the product [2]. Apart from microbial spoilage, the most common cause of these sensory changes in meat and meat products that can lead to consumer rejection is oxidation, which usually produces harmful reactive oxygen species (ROS) and reactive nitrogen species (RNS), such as superoxide, hydrogen peroxide, singlet oxygen, and nitric oxide free radicals [3]. Beef contains high-quality protein and amino acids for our bodies [4]. During the curing process, under the action of endogenous

☆ Yingyang zhang reports financial support was provided by the Science and Technology Project Plan of the Science and Technology Project of Jiangsu Province. Yingyang zhang reports financial support was provided by the Science and Technology Project of Changzhou. If there are other authors, they declare that they have no known competing financial interests or personal relationships that could have appeared to influence the work reported in this paper.

* Corresponding author.
E-mail address: chenwentao0608@outlook.com (C.H.E.N. Wen-Tao).

https://doi.org/10.1016/j.heliyon.2024.e24515
Received 30 December 2022; Received in revised form 5 January 2024; Accepted 10 January 2024
Available online 11 January 2024
2405-8440/

peptidase, the protein in beef is further hydrolyzed into active peptides. Usually, these active peptides have many biological activities [5], such as antihypertensive, antioxidant, bacteriostatic, and anticancer activities [6]. Bioactive peptides [7] are hidden in the primary structure of proteins, but when proteins are affected by enzymes, acids, or bases, they are hydrolyzed to obtain bioactive peptides. Many studies have identified bioactive peptides from different types of meat. Chen [8] isolated two peptides from rabbit meat with ACE inhibitory activity. Lee [9] purified LIVGIIRCV from beef myofibrillar protein, which has an effective antihypertensive effect. As a means of preservation, dry-cured meat [10] has a long history in China. During the production process, enzymes hydrolyze proteins into bioactive peptides. Wang [11] isolated the antioxidant peptides FWIE and APYMM from Chinese dry-cured mutton ham. Alejandro [12] confirmed the ACE activity of the dipeptide Ala-Ala (AA) in dry-cured ham.

Computer biology is a rapidly evolving field that includes the theory, programming, and application of computational methods to model, predict, and elucidate biological functions at the molecular level [13]. Today, a wide variety of biomolecular simulation methods are available for a variety of problems in structural biology. Tools such as molecular docking are biomolecular simulation methods based on integrated bioinformatics analysis, which examine the interactions between molecules, such as proteins and peptides, and predict their binding patterns and affinity at the molecular or atomic level through computer programming. These theoretical simulation strategies have been widely used in drug discovery research and virtual screening studies dedicated to finding novel active biomolecules, such as bioactive peptides. In bioactive peptides, molecular docking allows the characterization of peptide behavior at target protein-binding sites [14]. Since molecular docking is a structure-based approach [15], it can characterize the structure-activity relationship of peptides. In general, the molecular docking process involves predicting the molecular orientation of the ligands in the recipient and then calculating their complementary interactions using a scoring function (i.e., binding affinity). Shen [16] used molecular docking for the study of three umami peptides of L. C. wild-born that can be embedded in the binding pocket of the taste receptor T1R3 cavity. By combining Python script calls, Zhang [17] realized batch processing of molecular docking and screened 208 potential umami peptides from 20 peptides identified in chicken soup.

Superoxide dismutase (SOD) [18] is the only known enzyme that directly scavenges free radicals and maintains the redox balance by catalyzing the rapid conversion of superoxide anions into molecular oxygen and hydrogen peroxide. SOD widely exists in animals and plants. Since it was first isolated from bovine red blood cells in 1938, research on the SOD enzyme has been conducted for more than 70 years. Through the separation and purification of dry-cured beef active peptide (BPH), this experiment identified the antioxidant peptide FDGDF and combined it with ultraviolet, visible spectrum [19], fluorescence spectrum [20], and FT-IR spectrum [21], discussing the change rule of antioxidant peptide FDGDF and superoxide dismutase SOD. The binding site and force field analysis of FDGDF and SOD were simulated by quantum chemical simulation [22]. The binding and dissociation rates of SOD and FDGDF were determined by an SPR biological force analyzer [23]. The antioxidant potential of the polypeptide FDGDF was found through experiments, which provided research for the further development of beef products.

2. Materials and methods

2.1. Materials

SOD, DPPH, NBT, PMS, and NADH were purchased from Aladdin Biological Reagents Co., LTD. (Shanghai, China); all were analytical grade.

2.2. Process of dry-cured beef

The following traditional dry salted beef method was adopted for curing. The beef tenderloin (*psoas major* muscle) meat (purchased from Yonghui Supermarket, Changzhou, Jiangsu Province) was cut into 300 g each (2.5 cm thick steaks) and cured for 5 days according to 5 % edible salt, 90 % relative humidity, and 3–5 °C. Then, the meat was marinated for 5 days at 12 °C and 80 % relative humidity. The body weight decreased by 45 % after curing for 7 days at 20 °C and 70 % relative humidity. Finally, the meat was marinated for 30 days at 22.5 °C. The sampling time was 0, 5, 10, 17, 32, and 47 days of curing.

2.3. Extraction of beef active peptide (BPH)

Samples (150 g) from each storage period were chopped and homogenized with 450 mL of 0.01 M HCL for 8 min. Centrifuge the homogenate at 4 °C and 12000×*g* for 20 min and filter it with double-layer filter paper. Then, 3 times the volume of ethanol was added, and the sample was kept at 4 °C for 20 h to precipitate the protein. After that, the sample was centrifuged at 4 °C and 12000×*g* for 10 min. The excess solvent was removed from the supernatant in the rotary evaporator and then freeze-dried. The freeze-dried powder was stored at −20 °C [24].

2.4. Antioxidant study

2.4.1. DPPH scavenging activities

DPPH scavenging activity was determined as described by Cai [25] with some modifications. For this purpose, BPH samples from different curing periods were dissolved in sterile water to prepare a crude peptide solution with a mass concentration of 1 mg/mL. Then, 2 mL of 0.2 mM/L DPPH free radical solution (dissolved in 95 % ethanol) was added to 2 mL of the sample, mixed well, kept at room temperature in the dark for 30 min, and the sample absorbance was measured at an A517 nm wavelength. The blank was 2 mL of the sample plus 2 mL of 95 % ethanol, and the control was 2 mL of DPPH plus 2 mL of 95 % ethanol. The DPPH scavenged activities (%) can be calculated using the following equation:

$$DPPH\ scavenged\ activities(\%) = \frac{(Ab - As)}{Ab} \times 100\%$$

where.

As: absorbance of sample.

Ab: absorbance of blank.

2.4.2. · OH free radical scavenging activities

According to the TIAN method [26], BPH from different curing periods was dissolved in sterile water to prepare a crude peptide solution with a mass concentration of 1 mg/mL. The mixture consisted of 4 mL of 1,10-phenanthroline (5 mM) and 4 mL of $FeSO_4$ (5 mM), and then 3 mL of phosphate buffer (pH 7.4) was added. After that, 3 mL of H_2O_2 (0.01 %) and 4 mL of crude peptide (1 mg/mL) were added. Finally, the mixture was placed at 36 °C for 1 h, and the absorbance was measured at A536 nm. Control: distilled water was used instead of polypeptide solution, and other reagents were the same as the sample. Blank: distilled water instead of H_2O_2 and other reagents were the same as the sample. The following formula was used to determine the result:

$$\cdot \mathrm{OH\ \ free\ radical}\ scavenged\ activities(\%) = \frac{(As - Ac)}{(Ab - Ac)} \times 100\%$$

where.

As: absorbance of the sample.

As: absorbance of control.

Ab: absorbance of blank.

2.4.3. ABTS⁺ free radical scavenging activities

BPH from different curing periods was dissolved in sterile water to prepare a crude peptide solution with a mass concentration of 1 mg/mL. Five milliliters of 7 mM ABTS solution was mixed with 88 mL of 140 mM potassium persulfate solution, placed at 20 °C for 20 h, and added to approximately 3 times 75 % ethanol (v/v). The absorbance at A734 nm was 0.70 ± 0.02 to obtain $ABTS^+$ free radicals. The sample consisted of 9.8 mL of diluted $ABTS^+$ free radical solution and 0.2 mL of 1 mg/mL crude peptide. The mixture of 0.2 mL distilled water, 9.8 mL diluted $ABTS^+$ free radical solution was used as a blank, and 1 mg/mL crude peptide 0.2 mL and 9.8 mL distilled water were used as controls. All mixtures were placed at room temperature for 0.5 h and measured at A734 nm with a spectrophotometer. The free radical scavenging activity formula of $ABTS^+$ is WANG [27]:

$$ABTS+\ \mathrm{free\ radical}\ scavenged\ activities(\%) = \frac{[Ab - (As - Ac)]}{Ab} \times 100\%$$

where.

As: absorbance of the sample.

As: absorbance of control.

Ab: absorbance of blank.

2.4.4. · O_2^- free radical scavenging activities

Refer to LAIGHT [28] for the method. BPH from different curing periods was dissolved in sterile water to prepare a crude peptide solution with a mass concentration of 1 mg/mL. The specific method was as follows: 1.5 mL of crude peptide solution, 0.5 mL of 300 mM NBT (pH 8.0 Tris HCl buffer solution configuration), 0.5 mL of 468 mM NADH (pH 8.0 Tris HCl buffer configuration), and 0.5 mL of 60 mM PMS (pH 8.0 Tris HCl buffer solution configuration) were added, mixed well, and kept at 25 °C in a water bath for 5 min. The absorbance value was measured at an A560 nm wavelength, and the buffer solution was used instead of the sample as the blank control. The · O_2^- free radical scavenging activities (%) were calculated according to the following formula.

$$\cdot O\_(2)\hat{(}\text{-}\ free\ radical\ scavenged\ activities(\%) = \left(1 - \frac{As}{Ab}\right) \times 100\%$$

where.

As: absorbance of the sample.

Ab: absorbance of blank.

2.5. Peptide separation

BPH was extracted from dry corned beef, which has 5 % salt during the curing process. The presence of buffer salt will cause damage to the column [29]: (1) column pressure increase; (2) column efficiency decrease; (3) the retention time of the same compound changes, taking an appropriate amount of sample and using a C18 desalting column to remove salt [30]. After peptide separation, salt and buffer were removed using the C18 column, which is the ideal substrate for trapping hydrophobic peptides. The peptide was bound to the reverse-phase column in a high aqueous mobile phase, the salt and buffer were washed away, and then the peptide was eluted with a high organic mobile phase. According to the antioxidant test results, BPH was selected for separation and purification, and Sephadex G-25 and Sephadex G-15 were chosen for two separate purifications. Sephadex G-25 separation and purification conditions: A 26 mm × 1 m chromatographic column was selected, distilled water filtered at 45 nm was used as the eluent for elution, and the flow rate was adjusted to 0.5 mL/min. Five milliliters of eluent was collected in each tube for the antioxidant performance test. The collected solution with good antioxidant performance was selected for secondary separation and purification of Sephadex G-15 and antioxidant capacity testing. The conditions were the same as those for Sephadex G-25.

Nano HPLC–MS/MS analysis [30]: Analyze the sample via LC–MS/MS, which is equipped with an online sodium jet ion source. The system was a Q Executive of series EASY nano LC 1200 ™ Plus mass spectrometer (Thermo Fisher Scientific, MA, USA). A 5 μL sample was loaded (analytical column: Acclaim Pep Map C18, 75 mm × 25 cm), and the sample was separated with a 60 min gradient. The column flow rate was controlled at 300 nL/min; the column temperature was 40 °C, the electric spray voltage was 2 kV, and the gradient started from 2 % of phase B, increased to 35 % in 47 min with a nonlinear gradient, increased to 100 % in 1 min, and maintained for 12 min. The mass spectrometer operates in the data-dependent acquisition mode and automatically switches between MS and MS/MS acquisition. The mass spectrum parameters were set as follows: (1) MS: scanning range (m/z): 200 1800; Resolution: 70000; AGC target: 3e6; Maximum injection time: 50 ms; (2) HCD-MS/MS: resolution: 17500; AG Ctarget: 1e5; Maximum injection time: 45 ms; Collision energy: 28; Dynamic exclusion time: 30 s.

2.6. Antioxidation mechanism research

2.6.1. UV–visible spectroscopy

The concentration of SOD (purchased from Aladdin Biological Reagent Co., Shanghai, China) was 1.0×10^{-6} mol (prepared with 0.05 mol PBS buffer solution of pH 7.8), FDGDF was added at different concentrations (synthesized by Nanjing Jinsirui Biotechnology Co., Ltd., >99 %, Nanjing, Jiangsu), the ultraviolet absorption spectrum of 200~350 nm was scanned with the corresponding concentration of SOD as the reference, and the change rule of the SOD-FDGDF system was studied at different temperatures (15 °C, 25 °C, 35 °C).

2.6.2. Fluorescence spectrum

The concentration of SOD was 1.0×10^{-6} mol (prepared with 0.05 M PBS buffer solution with pH 7.8), and FDGDF was added at different concentrations. SOD at the corresponding concentrations was used as a reference, the excitation wavelength was set at 280 nm, and the excitation and emission slits were 5 nm. At different temperatures (15 °C, 25 °C, 35 °C), the emission spectra of the 300–500 nm reaction system were scanned, and the fluorescence reaction of FDGDF to SOD was studied.

2.6.3. FTIR test

The concentration of SOD was 1.0×10^{-6} mol (PBS buffer of 0.05 M with pH 7.8 was used), and the background test was carried out with PBS buffer. SOD enzyme droplets with different concentrations of FDGDF were added to the KBr tablet to collect data. Secondary structures of 1600 cm-1~1700 cm^{-1} were analyzed at peak fit.

2.6.4. SOD activity detection

The SOD enzyme activity test kit was purchased from Nanjing Jiancheng Bioengineering Research Institute (Nanjing, Jiangsu), and the specific test methods refer to the instructions.

2.6.5. Molecular docking

The superoxide dismutase (SOD) protein structure (PDB, ID:1PU0 [31]) was predicted using AlphaFold2 [32], and the three-dimensional structure of the polypeptide (1-FDGDF-5) was also predicted using AlphaFold2. A hydrogen atom was added using UCSF Chimera software [33], AMBER14SB charge was assigned by SOD protein, and the protonation state was treated under neutral conditions using the H^{++}3.0 program [34]. The FDGDF used the Gaussian 09 software package [35] to perform conformation optimization and single point energy calculation on the B3LYP/6-31G base set and then used Multiwfn software [36] to calculate RESP charge while using Multiwfn's density functional Reactivity theory (DFRT) module for Fukui function calculation. Nucleophilic electrophilic calculations were performed for each atom, and then HUMO and LUMO calculations were performed for the B3LYP/6-31G group. Autodock 4.2 was used for molecular docking [37], the SOD protein was set to the flexible docking configuration of the site, and the genetic algorithm was used for global search docking. The but box size was set to 45 Å, and the spacing step was set to 0.375. The maximum limit of the conformation search was set as 10000. A genetic algorithm was used for conformation sampling and scoring, and the optimal conformation was selected by conformation sorting according to docking scores [38].

2.6.6. SPR biological force analysis

For protein polypeptide samples, the direct coupling method was suitable for testing. Specifically, SOD protein was coupled to the surface of the CM5 chip by amino coupling (the coupling amount of SOD was 5300 RU, finally meeting the test requirements, and the expected Rmax was 58.7 RU). FDGDF passed through the chip as the analysis material and the signal changes were observed. The concentration gradient of FDGDF used in this experiment was 200, 100, 50, 25, and 12.5 M. According to the signal curve, the binding mode of SOD protein and FDGDF was fast binding and fast dissociation. Steady-state fitting was used for analysis [27].

3. Results and analysis

3.1. Extraction of BPH

Based on the standard curve for bovine serum protein, y = 0.1281x-0.0002 (R^2 = 0.9997), the crude peptide content in samples with different processing times could be calculated, as shown in Fig. 1 (A). The BPH content increases with the curing time. In the unprocessed period, the BPH content was approximately 1.50 mg/mL, and it increased to 1.85 mg/mL after 47 days of pickling, representing a 23.33 % increase. On the 10th day, protein hydrolysis was relatively strong, resulting in an increase of approximately 0.25 mg/mL in BPH content.

Proteins have a wide range of functional properties in organisms, including their ability to form networks and structures and react with water, salt, and other components; this plays a crucial role in the formation of meat texture, sensory properties, and nutritional quality. Protein hydrolysis occurs during the meat fermentation process [24]. The main structural proteins in meat, such as actin, myosin, and collagen, undergo hydrolysis by endogenous peptidases [39] (mainly cathepsin and calpain), breaking down complete proteins into small peptides. The release of exogenous peptides further degrades these small peptides into single amino acids, dipeptides, or tripeptides.

Regarding the glycine standard curve, y = 0.0135x - 0.0154 (R^2 = 0.9999), refer to Fig. 1 (B) to determine the number of peptide chains in different periods. After the curing process, the average peptide chain length increased by 45.88 %. Based on the average molecular weight of each amino acid, which is 126.7 Da, the average molecular weight of the BPH peptide chain after 47 days of curing was 2.66 kDa.

3.2. Antioxidant activity

There are several indicators used to assess antioxidant activity, including DPPH, ·OH, $ABTS^+$, and $\cdot O_2^-$ free radical scavenging performance. In this experiment we employed these indicators to evaluate antioxidant activity. DPPH radical scavenging activity is often used to gauge the antioxidant activity of natural extracts. In this study, BPH exhibited robust DPPH radical scavenging activity. As depicted in Fig. 1 (C), BPH on Day 47 demonstrated a 15.86 % increase in DPPH radical scavenging activity compared to Day 0.

DPPH is a stable free radical, but it can be quenched through electron transfer and hydrogen atom transfer reactions [40]. Among these two quenching mechanisms, electron transfer reactions are notably fast and not dependent on diffusion. Consequently, the variance in DPPH radical scavenging activity of BPH might be attributed to the extension of fermentation time. With enzymatic hydrolysis, large protein molecules are further broken down into smaller active peptide molecules [41]. BPH at 47 days may possess smaller molecular weights, and DPPH radical scavenging activity primarily relies on hydrogen atom transfer. Unlike DPPH, ·OH is the most potent free radical and can react with the most active peptides. ·OH boasts a high reduction potential, and some antioxidants with substantial electron transfer capability can neutralize ·OH [42]. In this study, the scavenging rate of ·OH free radicals increased from Days 0–10, but a significant increase was observed from Days 10–47. $ABTS^+$ radical scavenging activity is a valuable measure for evaluating active peptides. $ABTS^+$ radicals engage in two primary quenching mechanisms [43]: electron transfer and hydrogen atom transfer reactions. As indicated by Fig. 1 (C), BPH exhibited high $ABTS^+$ radical scavenging activity, likely because BPH possesses strong electron transfer and hydrogen atom transfer abilities. This finding aligns with the clear empirical findings observed for DPPH radicals. $\cdot O_2^-$ free radicals can promote oxidation reactions to generate hydrogen peroxide and hydroxyl radicals. The test results for $\cdot O_2^-$ free radical scavenging indicated that BPH had significantly increased scavenging rates [44]. Compared to BPH at 47 days, the scavenging rate of $\cdot O_2^-$ free radicals on Day 0 increased by approximately 14.45 %, potentially due to the enhanced electron transfer ability of the smaller molecule BPH.

Through antioxidant testing of BPH at various time points, it was observed that its antioxidant capacity significantly increased after 10 days. The scavenging rate of 1 mg/mL BPH for DPPH free radicals at 47 days increased by 11.47 %, that of ·OH increased by 4.25 %, that of $ABTS^+$ increased by 5.32 %, and that of $\cdot O_2^-$ increased by 8.89 % compared to 10 days.

3.3. Separation of FDGDF

Peptides usually consist of 3–20 amino acid residues, and their biological activity is determined by the composition and sequence of

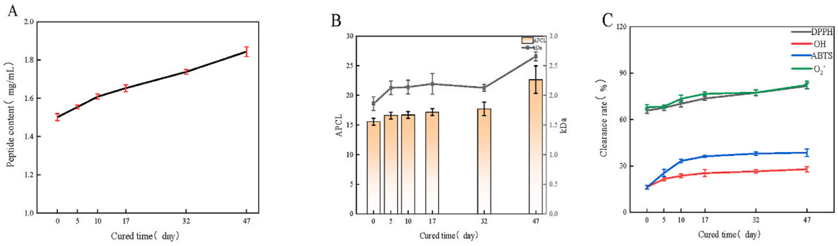

Fig. 1. Peptide content and peptide analysis of dry corned beef at different periods (A-Peptide content, B-APCL, C-clearance rate).

amino acids [45]. Many natural proteins are enzymatically hydrolyzed to produce peptides with diverse biological activities. To study these peptides, it is essential to understand their structure and sequence, which necessitates purification.

In the process of identifying bioactive peptides, the initial step involves extracting peptides from the source organism. Subsequently, unique bioactive peptides are screened from the extract, and various separation techniques are employed to isolate individual pure peptides. These separation methods encompass membrane separation, ion exchange chromatography, reversed-phase high-performance liquid chromatography, and gel chromatography, among others. Each technique has its own set of advantages and limitations.

In this particular study, gel chromatography was utilized to separate BPH. Gel chromatography is effective for separating both peptides and proteins based on differences in molecular size. Smaller molecules tend to enter the gel matrix and have longer retention times, while larger molecules pass through more quickly. The choice of gel type is crucial for separating molecules of varying molecular weights. In this experiment, Sephadex G-25 and Sephadex G-15 were selected for separation and purification. Sephadex G-25 (Fig. 2A) is typically used for the separation of macromolecular proteins or peptides in the range of 1000–5000 Da, while Sephadex G-15 (Fig. 2B) is suitable for peptides under 1500 Da.

As shown in Fig. 2-A, BPH was separated and purified by Sephadex G-25. Its OD value was tested at A220 nm. Six components were separated, and each component was tested for antioxidant activity. The results showed that the antioxidant activity of component C was higher than that of the other five components. The DPPH free radical scavenging rate of component C was 63.33 %, the $\cdot O_2^-$ free radical scavenging rate was 64.52 %, which was significantly higher than that of the other five components, and the ·OH scavenging rate was 15.91 %, which was slightly higher than that of the other components. The ABTS$^+$ clearance rate of component C was 34.93 %, slightly lower than that of component D (37.64 %); this may be because the electron transfer capacity of the peptide in component C was slightly lower than that of the peptide in component D, but the clearance rate of the other three components was higher than that of other components, so component C was selected for reseparation.

Sephadex G-15 has a smaller pore size than Sephadex G-25, so it is commonly used to repurify peptides. As shown in Fig. 2-B, the components were collected according to the elution volume once every 5 mL. The collected components are tested for their OD values at A220 nm, and the results show that there are five collection peaks: 45 mL of C1; 145 mL of C2; 240 mL of C3; 325 mL of C4; and 415 mL of C5. These components were tested for their antioxidant capacity, and the results showed that the antioxidant capacity of C2 was better than that of the other four components. The characteristics of the results were found through the analysis of the C2 mass spectrum, combined with BLAST, Peptide Ranker, and PDB searches (Table 1).

After peptide sequence analysis and PDB search, the analysis results show that C2-2 may be produced by the hydrolysis of P02465 collagen, C2-3 may be produced by the hydrolysis of P01966 bovine hemoglobin, and C2-1, C2-4, and C2-5 are not retrieved in the PDB of the bovine organism. This is possibly because these three components are produced by the condensation of hydrolyzed short peptides or are sequences in other organisms, and their sequences were not successfully retrieved in PDB. The prediction of Peptide Ranker's biological activity shows that the C2-2 component has the strongest biological activity. As shown in Fig. 2-C, through the 1 mg/ml antioxidant test, the results showed that the C2-2 component had the strongest antioxidant activity, which was consistent with the prediction results of the peptide ranking. Therefore, FDGDF was selected to study the antioxidation mechanism.

The identification of polypeptides was completed by Shanghai Easy Computing Biotechnology Co., Ltd. (Shanghai, China). After analyzing BPH in six different periods, we found that the hydrolysis of P02465 may produce FDGDF. The production process is as follows: under the action of endogenous peptidase, collagen P02465 first hydrolyzes to generate FDGDFYRA short peptide, and after 17 days, the peptide chain continues to hydrolyze, breaking the FDGDFYRA peptide chain and generating FDGDF. Using RCSB PDB and NCBI to analyze the FDGDF generation process, Fig. 3 was created using PYMOL. The information on FDGDFYRA and FDGDF is shown in Table 2. FDGDF is produced by further hydrolysis of FDGDFYRA on the 10th day of curing.

3.4. Antioxidation mechanism research

SOD can directly participate in the elimination of free radicals in organisms. Previous studies have focused on the extraction and identification of antioxidant peptides. There are few studies on the interaction between SOD and antioxidant peptides at the molecular level. Ultraviolet–visible absorption spectroscopy and fluorescence spectroscopy [20] can analyze the type of interaction between large molecules and small molecules of proteins and analyze the changes in protein conformation, which is an important method to study the interaction between molecules. FT-IR [21] can characterize the secondary structure changes before and after protein binding

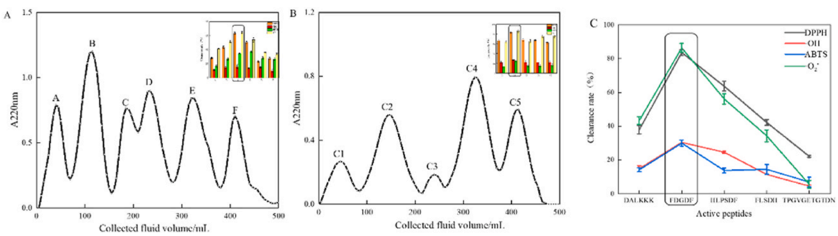

Fig. 2. Separation of BPH components by Sephadex G-25 and Sephadex G-15
(A-Sephadex G-25, B- Sephadex G-15, C-Active peptides).

Table 1
Analysis results of the main components of C2

Component	Active peptides	Length	*m/z*	PI	Peptide Ranker	PDB
C2-1	DALKKK	6	351.7298	9.70	0.11879	–
C2-2	FDGDF	5	600.2304	3.56	0.94884	P02465
C2-3	HLPSDF	6	715.3425	5.08	0.70577	P01966
C2-4	FLSDH	5	618.2899	5.08	0.49431	–
C2-5	TPGVGETGTDN	11	1047.461	3.67	0.07140	–

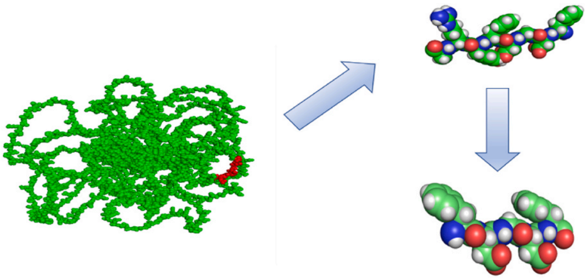

Fig. 3. Simulation of hydrolysis (PDB ID: P0465) hydrolysis to produce FDGDF.

Table 2
Comparison of FDGDFYRA and FDGDF.

Peptide	Mass	Length	ppm	*m/z*	RT	Source
G.FDGDFYRA.D	989.4243	8	1.2	990.4327	28.45	0,5,10,17,32,47
G.FDGDF.Y	599.2227	5	0.7	660.2304	30.50	10,17,32,47

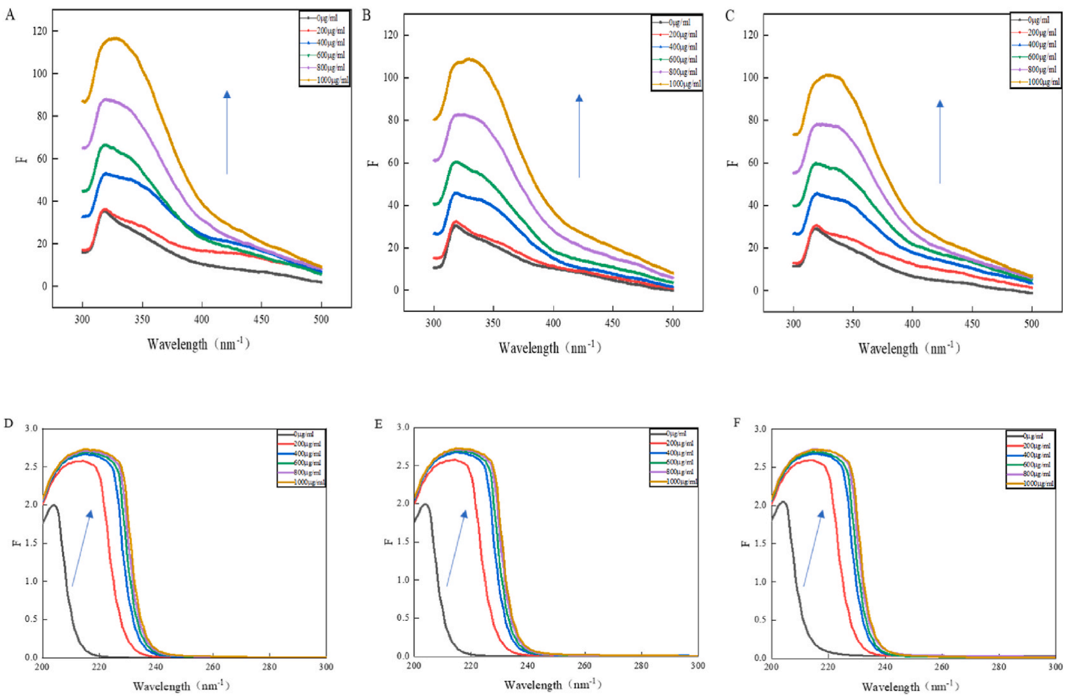

Fig. 4. UV–visible spectrum and fluorescence spectrum of SOD combined with FDGDF (A, B, C-UV−visible spectrum, D, E, F- fluorescence spectrum).

with small molecules by analyzing its 1600 cm^{-1}~1700 cm^{-1}. Due to the complex spatial structure of proteins after binding with antioxidant peptides, it is a great challenge to accurately obtain the active sites and electron transfer pathways of FDGDF and SOD by experimental methods. The quantum chemical simulation method has significant advantages; it can predict its binding sites by a simulation method and predict its spatial structure and structure-activity relationship with an SPR biological force analyzer.

The SOD enzyme was set in a pH 7.8, 0.05 mol/L PBS buffer solution with a concentration of 1.0×10^{-6} mol. Different concentrations of the antioxidant peptide FDGDF (0 μg/mL, 200 μg/mL, 400 μg/mL, 600 μg/mL, 800 μg/mL, 1000 μg/mL) were added, and UV–visible (Fig. 4-A, B, C) and fluorescence spectra (Fig. 4-D, E, F) were tested at different temperatures (15 °C, 25 °C, 35 °C). In the 200–300 nm UV–visible spectrum, the SOD enzyme displayed a strong absorption peak at A225 nm. This absorption peak exhibited a redshift with increasing FDGDF concentration, and this trend was consistent at different temperatures. This redshift might be attributed to electronic transitions [46] occurring upon the combination of FDGDF and SOD, leading to the observed shift in the absorption peak.

The fluorescence spectrum test revealed that the fluorescence spectrum experienced a redshift as more FDGDF was added, with variations observed at different temperatures. The increased fluorescence intensity could be attributed to changes in the original secondary structure of SOD caused by the interaction between FDGDF and SOD. This interaction likely led to a spatial separation of the fluorescent group and the fluorescent quenching agents, such as sulfur groups, cysteine, and disulfide bonds [47], within SOD. This separation resulted in an increase in the fluorescence intensity of SOD [48]. Fig. 5 (A, B, C) depicts the changes in the secondary structure of FDGDF and SOD enzymes, as analyzed by Peak Fit (Fig. 5-D, E, F). FT-IR spectra showed that the addition of FDGDF caused varying degrees of changes in the secondary structure, including a decrease in the α-helix and an increase in the β-sheet structure.

To further study the structure-activity relationship between FDGDF and SOD, we used the SOD activity test box (purchased from Nanjing Jiancheng Institute of Biotechnology) by adding different amounts of FDGDF. As shown in Fig. 6, SOD activity increased with the addition of FDGDF. The activity of SOD without FDGDF was 16.24 %. Up to 400 μg/ml, the activity increased by 2.66 %. However, after reaching 400 μg/ml, the activity of SOD increased significantly and was 11.64 % higher than that without FDGDF. Therefore, we inferred that the spatial structure of the SOD enzyme changed after adding FDGDF. After the addition of FDGDF, the ultraviolet–visible light spectrum and fluorescence spectrum of SOD exhibited a redshift, and the β-fold increased significantly, indicating a change in the secondary structure [49]. Therefore, we concluded that FDGDF could increase SOD activity.

3.5. Molecular docking

Through molecular docking, we obtained the binding mode and action details of the polypeptides FDGDF and SOD. As shown in Fig. 7 below, the charge center of phenylalanine Phe5 in FDGDF formed a π-stacking interaction with Val113 on the SOD protein, and Ser111 formed a hydrogen bonding interaction with the carbonyl oxygen of the polypeptide glycidyl (G) acid. The amino group of the glycine amide bond of the polypeptide formed a hydrogen bond with the skeleton carbonyl oxygen of Arg108. Two aspartic acids (Asp,

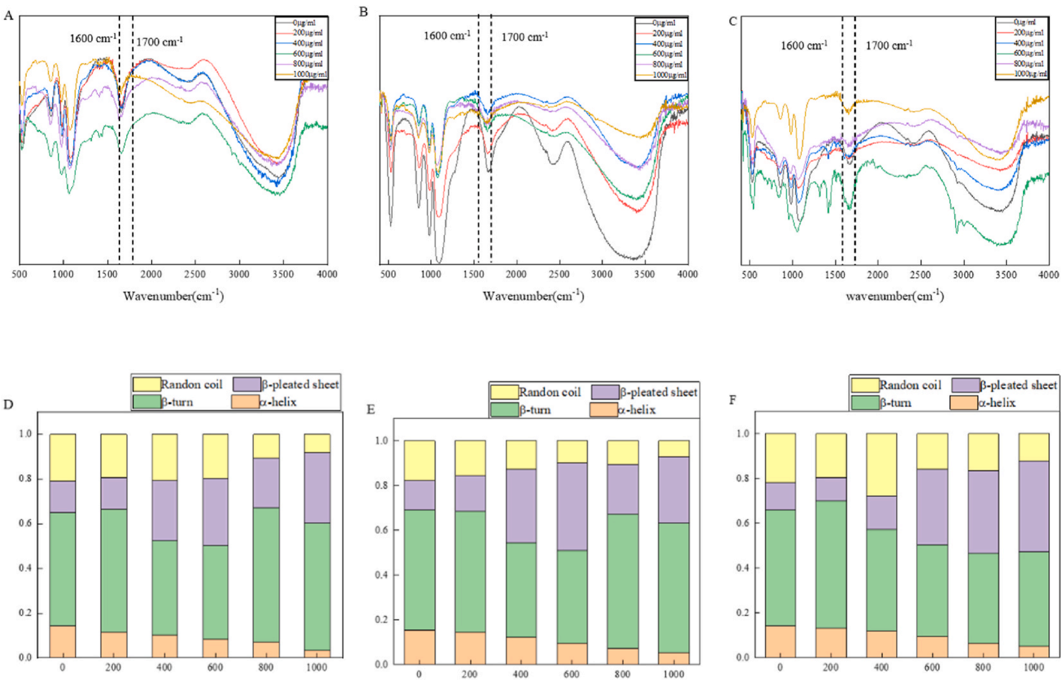

Fig. 5. SOD and FDGDF combined FT-IR analysis of the secondary structure (A, B, C- FT-IR, D, E, F- Peak Fit).

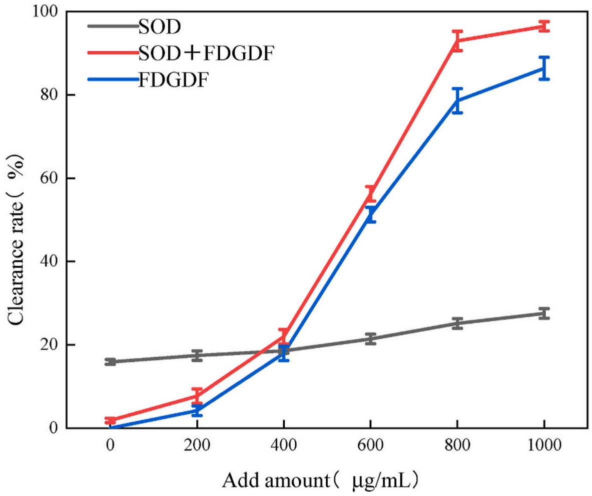

Fig. 6. Comparison of SOD activity.

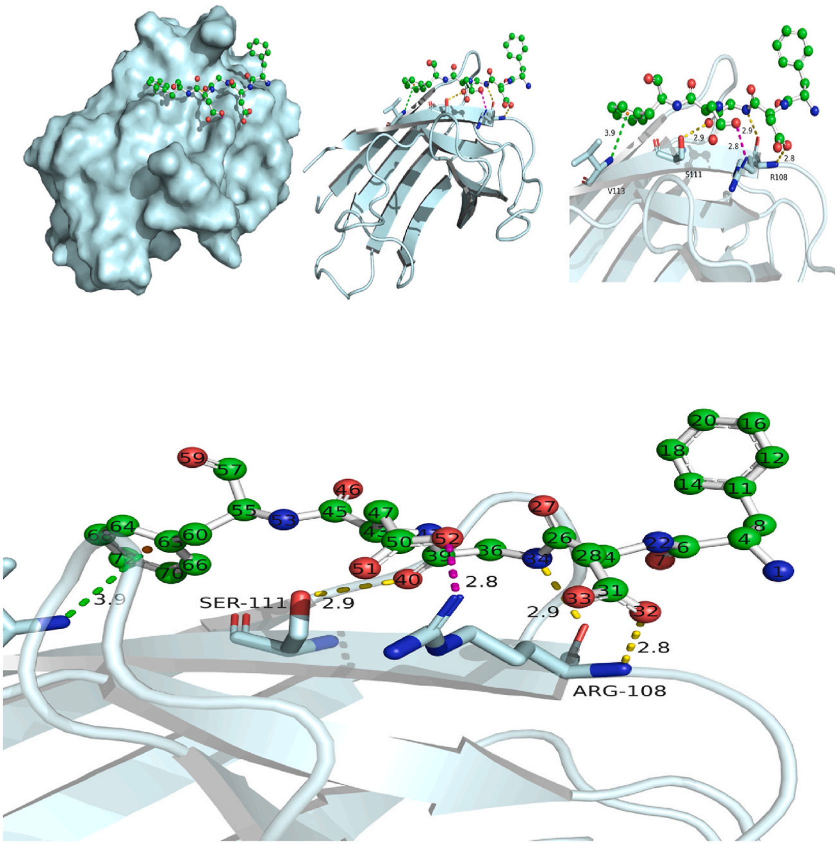

Fig. 7. SOD protein and peptide interaction binding pattern.

D) of FDGDF formed a salt bridge and hydrogen bond with Arg108, respectively.

FDGDF uses a ball-and-stick model to display C as green, O as red, N as blue, and SOD protein as light blue. Hydrogen bonding is shown as a yellow dotted line, salt bridge as a magenta dotted line, and π-stacking as a green dotted line. The details of their interaction were further analyzed, including bond length and bond energy. As shown in Fig. 7, the O40 atom of FDGDF participated in hydrogen bond formation, with a bond length of 3.9 Å and a bond energy of −1.9 kcal/mol. The O52 atom of asparagine participates in the salt bridge, with a bond length of 2.8 Å. The bond energy is −8.8 kcal/mol because the salt bridge is a combination of charge attraction and hydrogen bonding, so it has a high bond energy. The N34 atom on glycine participated in the formation of a hydrogen bond, with a bond length of 2.9 Å and a bond energy of −3.1 kcal/mol. The O32 oxygen atom on aspartic acid participated in the hydrogen bond with the skeleton amide of Arg108, with a bond length of 2.8 Å and bond energy of −4.0 kcal/mol, because of the close distance and the skeleton hydrogen bond. Therefore, it also has a high energy value.

From the analysis of action details (Table 3), the contribution of two aspartic acids to the binding energy is very large, one is −8.8 kcal/mol, and the other is −4.0 kcal/mol, which is higher than that of other amino acids. Phenylalanine has a long bonding distance, although it has a π-stacking effect with the α-carbon atom of the Val 112 skeleton. However, the energy contribution is only −1.9 kcal/mol.

Furthermore, the charge distribution of each atom of the peptide, the Fukui index, and the HOMO and LUMO properties of the peptide were analyzed using DFT calculations. Fig. 8 shows the HOMO and LUMO orbitals of the polypeptide molecules. HOMO is more relaxed in its electron binding and has the property of an electron donor or strong nucleophilic property, while LUMO has a strong affinity for electrons and has the property of an electron acceptor or electrophilic. These two orbitals are most likely to interact with each other. It plays an extremely important role in chemical reactions. Fig. 8 shows that the LUMOs are mainly concentrated on the two aspartic acids of FDGDF, indicating that these two amino acids have higher electron density and strong electron absorption ability or strong electrophilicity. The glycine carbonyl group in the middle of FDGDF also has a higher LUMO orbital distribution; in addition, the phenylalanine on the right also has a LUMO orbital distribution. From the above binding mode, these amino acids make more contributions to the binding and form more interactions, mainly salt bridges and hydrogen bonding. However, the molecular orbitals of phenylalanine 1, which were not involved in this study, were mainly due to the high HOMO distribution. By calculation, the LUMO value of FDGDF is −0.2369 Hartree, the HOMO is −0.2486 Hartree, and their gap is 0.0117 Hartree. The smaller the gap is, the stronger the activity, and the easier the reaction.

In this study, Gaussian was used to optimize the structure of FDGDF under the B3LYP/6-31G base set, and the open-source software package (Multiwfn) was used for charge calculation and Fukui index calculation. The RESP charge distribution results are shown in Table 4. The charge distribution indicates the density of the electron cloud. A negative charge indicates that the electron is dense, and the atom has a strong ability to attract electrons and has electrophilicity; a positive charge indicates that it can give electrons and has nucleophilicity. The data show that the above atoms involved in the reaction, such as O40, O52, O32, and N34, have charges of −0.4989, −0.4175, −0.4339, and −0.3985, indicating that these atoms have a strong ability to attract electrons, which is consistent with the HOMO-LUMO analysis.

Furthermore, the Fukui index was analyzed, and the results are shown in Table 5, where f0 represents the reactivity of atoms, and the larger the value is, the greater the possibility of participating in free radical reactions. The calculation showed that the f0 values of O32, O40, and O52 were 0.0699, 0.0164, and 0.076, respectively, with O32 and O52 having higher f0 values. O40 also has a value higher than the average of 0.013, indicating that these atoms are more likely to react. According to the binding mode, these atoms do indeed form key interactions, and their bond energies are higher.

Table 6 indicates that the electrophilicity values of the participating atoms O32, O40, and O52 were 1.8617, 0.9216, and 1.5541, respectively. The electrophilicity of O32 is the highest at 1.8617, while O52 has the largest nucleophilic value at 0.1967. These values are higher than those of most atoms, indicating that these atoms are more likely to participate in the reaction.

3.6. SPR biological force analysis

Surface plasmon resonance (SPR) is an optical biological sensing technology [45]. When light enters the optical medium from the optically dense medium, reflection and refraction occur, leading to a change in the SPR resonance angle based on the refractive index of the reflected light. When biomolecules are coupled on the sensor chip's surface and interact with other molecules, they cause a change in the refractive index of the reflected light. By continuously monitoring the shift in the SPR resonance angle, specific binding between the biomolecules on the SPR chip can be recorded. SPR enables the real-time monitoring of biomolecular interactions and provides information on intermolecular binding and dissociation due to its straightforward sample preparation and high sensitivity.

As illustrated in Fig. 9, when testing the combination of FDGDF and SOD at different concentrations (12.5 μM, 25 μM, 50 μM, 100 μM, 200 μM), it becomes evident that higher FDGDF concentrations result in stronger signals from the detector. At 200 μM, the signal is at its peak, and dissociation occurs rapidly, indicating fast-binding and fast-dissociation modes. Through steady-state fitting analysis of the affinity, the affinity constant was determined to be 1.217×10^{-4} M (121.7 μM).

4. Conclusion

As one of the meat products with a long history of human consumption, dry-cured products are rich in nutrients; however, their antioxidant mechanism remains unclear. In this experiment, the antioxidant peptide FDGDF, isolated from dry-cured beef, was combined with the SOD enzyme. The ultraviolet–visible, fluorescence, and FT-IR spectra showed that FDGDF could enhance the β-fold of the SOD enzyme. Molecular docking simulated the binding sites as Arg 141, Thr135, Ala 138, and Gly 139, with a binding energy of −6.7 kcal/mol, demonstrating an excellent binding effect. The binding and dissociation modes of FDGDF and SOD enzymes at different concentrations were analyzed using SPR biological force analysis, revealing a fast-binding and dissociation mode, with an affinity constant of 1.217×10^{-4} M (121.7 μM). A PDB search indicated that FDGDF is produced by the hydrolysis of P02465 collagen. The SOD activity detection kit indicated that FDGDF could improve SOD enzyme activity, effectively increasing it by 11.64 % at 1000 mg/ml FDGDF. In conclusion, the BPH antioxidant peptide FDGDF can enhance SOD activity by altering the secondary structure of SOD.

In this study, it was confirmed that FDGDF could enhance SOD activity in vitro through quantum chemistry. However, the

Table 3
SOD protein and peptide bond length and bond energy.

Keying type	Protein active sites	Peptide active site	Å	kcal/mol
π - Stacking	Val113	Benzene ring charge center (Phe5)	3.9	−1.9
Hydrogen bonding	Arg108	O32(Asp 2)	2.8	−4.0
Hydrogen bonding	Ser111	O40(Asp4)	2.9	−2.4
Salt bridge action	Arg108	O52(Asp4)	2.8	−8.8
Hydrogen bonding	Arg108	N34 (Gly 3)	2.9	−3.1

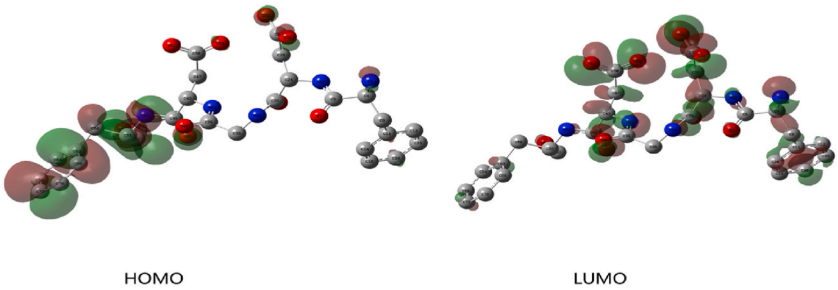

Fig. 8. Molecular orbital distribution of peptides, with HOMO of the highest occupied orbital on the left and LUMO of the lowest unoccupied orbital on the right.

Table 4
Local charge distribution for each atom of the polypeptide.

Atom	RESP charge
O32	−0.4339
N34	−0.3985
O40	−0.4989
O52	−0.4175

Table 5
Calculation results of the Fukui index.

Atom	q(N)	q (N+1)	q (N-1)	f-	f+	f0
O32	−0.2288	−0.3109	−0.1711	0.0577	0.0821	0.0699
N34	−0.0732	−0.0858	−0.077	−0.0038	0.0125	0.0044
O40	−0.2653	−0.306	−0.2732	−0.0078	0.0406	0.0164
O52	−0.202	−0.2705	−0.1186	0.0834	0.0685	0.076

Table 6
Electrophilicity and Nucleophilicity of atoms.

Atom	Electrophilicity	Nucleophilicity
O32	1.8617	0.1360
N34	0.2842	−0.0089
O40	0.9216	−0.0185
O52	1.5541	0.1967

experiment had some limitations. For instance, although the antioxidant peptide FDGDF was isolated, its specific hydrolysis pathway was not clear, and it could only be inferred to be produced by hydrolysis of collagen (PDB ID: P02465) during the curing process. Additionally, the hydrolysis pathway during the curing process remains unclear. While quantum chemistry and SPR biological force analysis verified that FDGDF can bind to the SOD enzyme in vitro to improve enzyme activity, the in vivo binding process may be affected by various factors (pH, temperature, enzymes, etc.), and in vitro testing cannot accurately represent the binding process in vivo. Therefore, it remains uncertain whether the in vivo binding process can enhance SOD enzyme activity. In conclusion, further exploration of the mechanism for improving enzyme activity by active peptides is necessary.

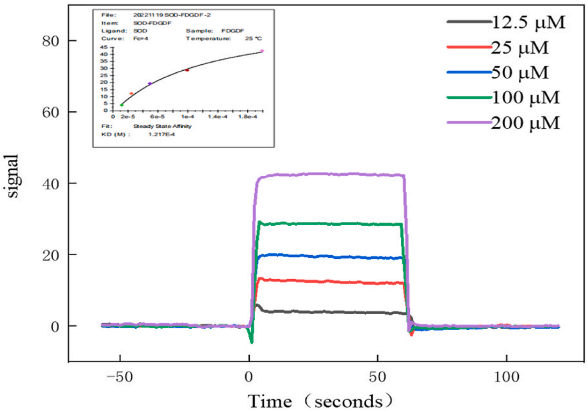

Fig. 9. SPR analysis of the interaction between FDGDF and SOD.

Funding

This work was financially supported by the Science and Technology Project Plan of the Science and Technology Project of Jiangsu Province (BY20212150) and the Science and Technology Project of Changzhou City (CE20202001).

Institutional Review Board Statement: Not applicable.

Informed Consent Statement: Not applicable.

Data availability

Data will be made available on request.

CRediT authorship contribution statement

C.H.E.N. Wen-Tao: Supervision, Data curation, Conceptualization. **Ying-Yang Zhang:** Investigation, Data curation. **Qiang Qiang:** Resources, Conceptualization. **Ping Zou:** Validation, Resources. **Ying Xu:** Formal analysis, Conceptualization. **Chengjun Sun:** Writing – review & editing. **Iftikhar Hussain Badar:** Validation, Conceptualization.

Declaration of competing interest

The authors declare the following financial interests/personal relationships which may be considered as potential competing interests.

References

[1] I.H. Badar, H. Liu, Q. Chen, et al., Future trends of processed meat products concerning perceived healthiness: a review, Compr. Rev. Food Sci. Food Saf. 20 (5) (2021) 4739–4778.
[2] R. DomíNGUEZ, M. Pateiro, M. Gagaoua, et al., A comprehensive review on lipid oxidation in meat and meat products, J]. Antioxidants 8 (10) (2019) 429.
[3] L.A. Videla, V. FernáNDEZ, Biochemical aspects of cellular oxidative stress, Arch. Biol. Med. Exp. 21 (1) (1988) 85–92.
[4] C.B. Jennifer, B. Gabriela, Oliveira, C.P.M. Maria, et al., Demand changes meat as changing meat reshapes demand: the great meat revolution, Meat Sci. 196 (2022) 109040.
[5] S. Guha, R.P. Ferrie, J. Ghimire, et al., Applications and evolution of melittin, the quintessential membrane active peptide, Biochem. Pharmacol. 193 (2021) 114769.
[6] T.M. Karpiński, A. Adamczak, Anticancer activity of bacterial proteins and peptides, Pharmaceutics 10 (2) (2018) 54.
[7] L. Kang, T. Han, H. Cong, et al., Recent research progress of biologically active peptides, Biofactors 48 (3) (2022) 575–596.
[8] J. Chen, X. Yu, W. Huang, et al., A novel angiotensin-converting enzyme inhibitory peptide from rabbit meat protein hydrolysate: identification, molecular mechanism, and antihypertensive effect in vivo, Food Funct. 12 (23) (2021) 12077–12086.
[9] S.Y. Lee, H.J. Kang, J.H. Kang, et al., Effect of emulsification on the antioxidant capacity of beef myofibrillar protein-derived bioactive peptides during in vitro human digestion and on the hepatoprotective activity using HepG2 cells, J. Funct.Foods 81 (2021) 104477.
[10] C. Liu, J. Wan, Y. Zhou, et al., Proteome profile of glycrol-mediated salt-reduction cured meat reveals the formation mechanism of eating quality, Food Chem. 382 (2022) 132395.
[11] J. Wang, M. Guo, Q. Wang, et al., Antioxidant activities of peptides derived from mutton ham, Xuanwei ham and Jinhua ham, Food Res. Int. 142 (2021) 110195.
[12] H. Alejandro, I. Yokoyama, M. Gallego, et al., Impact of oxidation on the cardioprotective properties of the bioactive dipeptide AW in dry-cured ham, Food Res. Int. 162 (2022) 112128.
[13] J. Zhang, X. Fu, L. Yang, et al., Neohesperidin inhibits cardiac remodeling induced by Ang II in vivo and in vitro, Biomed. Pharmacother. 129 (2020) 110364.
[14] Y. Zhang, X. Gao, D. Pan, et al., Isolation, characterization and molecular docking of novel umami and umami-enhancing peptides from Ruditapes philippinarum, Food Chem. 343 (2021) 128522.
[15] C. Li, Y. Hua, D. Pan, et al., A rapid selection strategy for umami peptide screening based on machine learning and molecular docking, Food Chem. 404 (2023) 134562.

[16] Q. Shen, L. Sun, Z. He, et al., Isolation, taste characterization and molecular docking study of novel umami peptides from Lactarius volemus (Fr.), Food Chem. 401 (2023) 134137.
[17] J. Zhang, J. Zhang, L. Liang, et al., Identification and virtual screening of novel umami peptides from chicken soup by molecular docking, Food Chem. 404 (2023) 134414.
[18] S. Stephenie, Y.P. Chang, A. Gnanasekaran, et al., An insight on superoxide dismutase (SOD) from plants for mammalian health enhancement, J. Funct.Foods 68 (2020) 103917.
[19] N.G. Hendricks, R.R. Julian, Leveraging ultraviolet photodissociation and spectroscopy to investigate peptide and protein three-dimensional structure with mass spectrometry, Analyst 141 (15) (2016) 4534–4540.
[20] M. Cavaco, C. PéREZ-Peinado, J. Valle, et al., To what extent do fluorophores bias the biological activity of peptides? A practical approach using membrane-active peptides as models, Front. Bioeng. Biotechnol. 8 (2020) 552035.
[21] A.T. Buddanavar, S.T. Nandibewoor, Multi-spectroscopic characterization of bovine serum albumin upon interaction with atomoxetine, Journal of pharmaceutical analysis 7 (3) (2017) 148–155.
[22] R.A. Friesner, M.-H. Baik, B.F. Gherman, et al., How iron-containing proteins control dioxygen chemistry: a detailed atomic level description via accurate quantum chemical and mixed quantum mechanics/molecular mechanics calculations, Coord. Chem. Rev. 238 (2003) 267–290.
[23] C. Williams, T.A. Addona, The integration of SPR biosensors with mass spectrometry: possible applications for proteome analysis, Trends Biotechnol. 18 (2) (2000) 45–48.
[24] L.-J. Xing, Y.-Y. Hu, H.-Y. Hu, et al., Purification and identification of antioxidative peptides from dry-cured Xuanwei ham, Food Chem. 194 (2016) 951–958.
[25] J. Cai, L. Xing, W. Zhang, et al., Selection of potential probiotic yeasts from dry-cured xuanwei ham and identification of yeast-derived antioxidant peptides, Antioxidants 11 (10) (2022) 1970.
[26] Y. Tian, X. Li, H. Xie, et al., Protective mechanism of the antioxidant baicalein toward hydroxyl radical-treated bone marrow-derived mesenchymal stem cells, Molecules 23 (1) (2018) 223.
[27] H. Wang, S. You, W. Wang, et al., Laccase-catalyzed soy protein and gallic acid complexation: effects on conformational structures and antioxidant activity, Food Chem. 375 (2022) 131865.
[28] D.W. Laight, T.J. Andrews, A.I. Haj-Yehia, et al., Microassay of superoxide anion scavenging activity in vitro, Environ. Toxicol. Pharmacol. 3 (1) (1997) 65–68.
[29] I.R. Smith, J.K. Eng, A.S. Barente, et al., Coisolation of peptide pairs for peptide identification and MS/MS-based quantification, Anal. Chem. 94 (44) (2022) 15198–15206.
[30] N.M. Sarbon, F. Badii, N.K. Howell, Purification and characterization of antioxidative peptides derived from chicken skin gelatin hydrolysate, Food Hydrocolloids 85 (2018) 311–320.
[31] J.L. Sussman, D. Lin, J. Jiang, et al., Protein Data Bank (PDB): database of three-dimensional structural information of biological macromolecules, Acta Crystallographica Section D: Biological Crystallography 54 (6) (1998) 1078–1084.
[32] J. Jumper, R. Evans, A. Pritzel, et al., Highly accurate protein structure prediction with AlphaFold, Nature 596 (7873) (2021) 583–589.
[33] E.F. Pettersen, T.D. Goddard, C.C. Huang, et al., UCSF Chimera—a visualization system for exploratory research and analysis, J. Comput. Chem. 25 (13) (2004) 1605–1612.
[34] R. Anandakrishnan, B. Aguilar, A.V. Onufriev, H++ 3.0: automating p K prediction and the preparation of biomolecular structures for atomistic molecular modeling and simulations, Nucleic Acids Res. 40 (W1) (2012) W537–W541.
[35] A. Frisch, Gaussian 09W Reference, Gaussian [J]. Inc, Wallingford, CT, USA, 2009.
[36] T. Lu, F. Chen, Multiwfn: a multifunctional wavefunction analyzer, J. Comput. Chem. 33 (5) (2012) 580–592.
[37] D.S. Goodsell, G.M. Morris, A.J. Olson, Automated docking of flexible ligands: applications of AutoDock, J. Mol. Recogn. 9 (1) (1996) 1–5.
[38] D.S. Goodsell, A.J. Olson, Automated docking of substrates to proteins by simulated annealing, Proteins: Struct., Funct., Bioinf. 8 (3) (1990) 195–202.
[39] C. Li, L. Mora, M. Gallego, et al., Evaluation of main post-translational modifications occurring in naturally generated peptides during the ripening of Spanish dry-cured ham, Food Chem. 332 (2020) 127388.
[40] W. Piang-Siong, P. DE Caro, A. Marvilliers, et al., Contribution of trans-aconitic acid to DPPH scavenging ability in different media, Food Chem. 214 (2017) 447–452.
[41] S. Kasamatsu, S. Komae, K. Matsukura, et al., 2-oxo-imidazole-containing dipeptides play a key role in the antioxidant capacity of imidazole-containing dipeptides, Antioxidants 10 (9) (2021) 1434.
[42] G. PéREZ-GonzáLEZ, V. MelíN, C. MéNDEZ-Rivas, et al., Role of a perhydroxyl radical in the chelator-mediated Fenton reaction, New J. Chem. 46 (10) (2022) 4884–4889.
[43] R. VAN DER Werf, C. Marcic, A. Khalil, et al., ABTS radical scavenging capacity in green and roasted coffee extracts, LWT–Food Sci. Technol. 58 (1) (2014) 77–85.
[44] Z. Duan, W. Duan, F. Li, et al., Effect of carboxymethylation on properties of fucoidan from Laminaria japonica: antioxidant activity and preservative effect on strawberry during cold storage, Postharvest Biol. Technol. 151 (2019) 127–133.
[45] M. Gallego, L. Mora, M.-C. Aristoy, et al., Evidence of peptide oxidation from major myofibrillar proteins in dry-cured ham, Food Chem. 187 (2015) 230–235.
[46] L. Joly, R. Antoine, A.-R. Allouche, et al., Ultraviolet spectroscopy of peptide and protein polyanions in vacuo: signature of the ionization state of tyrosine, J. Am. Chem. Soc. 129 (27) (2007) 8428–8429.
[47] R. Zhang, C. Jia, L. Zhao, et al., Characterization of the interaction between carbon black and three important antioxidant proteins using multi spectroscopy and modeling simulations, Chemosphere 222 (2019) 823–830.
[48] X. Hu, Z. Yu, R. Liu, Spectroscopic investigations on the interactions between isopropanol and trypsin at molecular level, Spectrochim. Acta Mol. Biomol. Spectrosc. 108 (2013) 50–54.
[49] Z. Cui, F. He, X. Li, et al., Response pathways of superoxide dismutase and catalase under the regulation of triclocarban-triggered oxidative stress in Eisenia foetida: comprehensive mechanism analysis based on cytotoxicity and binding model, Sci. Total Environ. 854 (2023) 158821.